Journal of Advanced Research (2017) **8**, 209–215

Cairo University

Journal of Advanced Research

ORIGINAL ARTICLE

Exfoliation of graphene sheets via high energy wet milling of graphite in 2-ethylhexanol and kerosene

Al-Sayed Al-Sherbini *, Mona Bakr, Iman Ghoneim, Mohamed Saad

Department of Measurements, Photochemistry and Agriculture Applications, National Institute of Laser Enhanced Science (NILES), Cairo University, P.O. Box 12631, Giza, Egypt

GRAPHICAL ABSTRACT

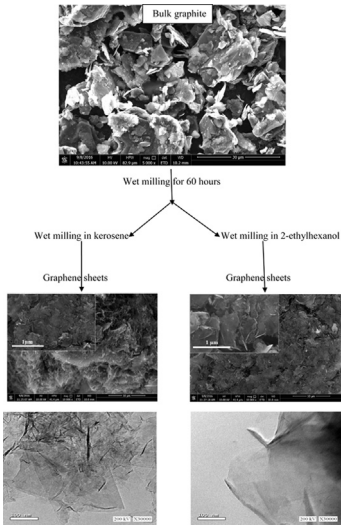

Abbreviations: XRD, X-ray diffraction; TEM, transmission electron microscopy; SEM, scanning electron microscopy; E-H, 2-ethylhexanol; K, kerosene.

* Corresponding author. Fax: +20 2 35708480.
E-mail address: elsayed@niles.edu.eg (A.-S. Al-Sherbini).

Peer review under responsibility of Cairo University.

Production and hosting by Elsevier

http://dx.doi.org/10.1016/j.jare.2017.01.004

ARTICLE INFO

Article history:
Received 29 November 2016
Received in revised form 25 January 2017
Accepted 26 January 2017
Available online 4 February 2017

Keywords:
Graphene
Wet ball milling
Kerosene
2-Ethyl-hexanol
Defects
Raman spectroscopy

ABSTRACT

Graphene sheets have been exfoliated from bulk graphite using high energy wet milling in two different solvents that were 2-ethylhexanol and kerosene. The milling process was performed for 60 h using a planetary ball mill. Morphological characteristics were investigated using scanning electron microscope (SEM) and transmission electron microscope (TEM). On the other hand, the structural characterization was performed using X-ray diffraction technique (XRD) and Raman spectrometry. The exfoliated graphene sheets have represented good morphological and structural characteristics with a valuable amount of defects and a good graphitic structure. The graphene sheets exfoliated in the presence of 2-ethylhexanol have represented many layers, large crystal size and low level of defects, while the graphene sheets exfoliated in the presence of kerosene have represented fewer number of layers, smaller crystal size and higher level of defects.

Introduction

Graphene is known as an atomic layer of graphite, which is also the essential unit for fullerenes and CNTs. It is a two dimensional (2D) crystal that is stable under ambient conditions [1,2]. Single sheets of graphene are expected to have tensile modulus and eventual strength values like those of single wall carbon nanotubes (SWCNTs) and have a vast electrical conductivity. Similar to SWCNTs, graphene sheets serve as fillers for the improvement of electrical and mechanical properties in composite materials [3]. Graphene has exceptional in-plane structural, mechanical, thermal and electrical properties. These properties make it attractive for application in many research fields [4,5].

Defects in graphitic materials are important for enhancing the performance of carbon-based materials for practical applications. Because of the high anisotropy of the mechanical strength or the electrical conductivity between the in-plane and out-of-plane directions [6]. For example, to avoid the slip of the graphitic plane with respect to its neighbors, orientational disorder of the graphite planes is useful, and it is essential for enhancing the average isotropic mechanical strength. The different types of defects can be investigated by Raman spectroscopy [7–12]. Carbon allotropes show their fingerprints under Raman spectroscopy typically by D, G, and 2D peaks around 1350 cm^{-1}, 1580 cm^{-1} and 2700 cm^{-1} respectively due to the change in electron bands. Identification of these features allows characterization of graphene layers in terms of number of layers present [13]. The integrated intensity ratio I_D/I_G for the D band and G band is widely used for characterizing the defect quantity in graphitic materials [13]. Although there are different synthesis methods of graphene, they can be simply classified into two categories: top down approach and bottom up approach [1]. The most well-known of these methods are mechanical exfoliation [10], electrochemical exfoliation [14,15], chemical-derived [16], chemical vapor deposition (CVD) [17,18], epitaxial growth on SiC [19], and arc discharge [20]. Graphene can also be produced by unzipping CNTs with strong oxidizing agents, laser irradiation or plasma etching [21]. Intercalation compound methods have also been used to obtain graphene through spontaneous exfoliation of graphite [22].

Mechanical milling has been employed for producing graphene via different ways that include the production of colloidal dispersion of graphene in organic solvent [23], the synthesis of functionalized graphene nanoplatelets by mechanochemical milling [24], the production of graphene through ball milling of graphite with oxalic acid dihydrate [25], the synthesis of graphene nanosheets via ball milling of pristine graphite in the presence of dry ice [26], and the production of graphene by using ball milling of graphite with ammonia borane [27]. The main goal of the present research is to employ the wet milling in the presence of kerosene and 2-ethyl-hexanol separately to process and manipulate graphite powder for producing graphene sheets in the powder form with tunable characteristics.

Experimental

Wet milling process was performed using a planetary ball mill (PM.100 CM, from Retsch, Haan, Germany), Hardened steel vial (500 cc), Hardened steel balls (5 mm in diameter). Graphite powders (Sigma Aldrich, <20 μm, Schnelldorf, Germany) were milled at which the weight of the milled graphite powders was 10 g, and the weight of the milling balls was 500 g, then, the ball to powder ratio was 50:1 (i.e. $B/P = 50$). The milling speed was 400 rpm, and the milling time was 60 h. The graphite powders were milled in the presence of both kerosene (commercially available, from ExxonMobil company, Cairo, Egypt), and 2-ethylhexanol ($\geqslant$99.6%, Sigma Aldrich, Saint Louis, MO, USA). The prepared samples were centrifuged at 5000 rpm for 20 min to be separated from the solvent. Heat treatment of the prepared samples was performed in a tube furnace under the flow of argon gas for 3 h at 600 °C. Structural characterizations were performed via X-ray diffraction (XRD- PANalytical's X'Pert PRO diffractometer, Almelo, Netherlands), and Raman spectroscopy (Bruker Senterra instrument, Ettlingen, Germany, with a laser of 532 nm). On the other hand, Morphological characteristics of graphite powders and the prepared graphene sheets were investigated by scanning electron microscopy (Quanta FEG 250 (FEI, Hillsboro, USA), and Transmission electron microscopy (TEM-JOEL-JEM-2100, Tokyo, Japan).

Results and discussion

Graphite layers are arranged to form bulk graphite via weak forces that well known as Van der Waals forces. These weak forces may resist the exfoliation of graphene from graphite via milling process. The impact and shear forces generated via high energy ball milling can overcome the Van der Waals forces between the graphite layers. These shear and impact forces can deliver an energy amount required to reduce the Van der Waals forces between the graphite layers and finally introduce facile exfoliation of the graphene sheets [26]. In the present work, the graphene sheets were exfoliated layer by layer from graphite according to the above mechanism that was enhanced via application of organic solvent as a milling environment to provide a great support for non-destructive exfoliation that was clearly observed with the samples.

The reason for using kerosene and 2-ethylhexanol as milling solvents for wet milling of graphite, is the high boiling point (~150 to 300 °C for kerosene, and 184 °C for 2-ethylhexanol). The high boiling point makes them suitable for milling of graphite for a long time (60 h), and high milling speed (400 rpm) using the planetary ball mill that well known as it has not a cooling system. Since the high milling speed for long time raises the mechanical energy applied to the sample, then the production of excessive heat is the result of these conditions, thereby the high boiling points of these solvents makes them as heat reducers during the milling process, and prevent further heating. Furthermore, the reason for the comparison between kerosene and 2-ethylhexanol as milling solvents for wet milling of graphite, is the difference in the viscosity of these solvents (10.3 centipoise for 2-ethylhexanol against 1.64 centipoise for kerosene), this difference in the degree of viscosity is an important factor to tune the shape, layers, and defects of exfoliated graphene. The number of collisions, the fracturing of the particles, and the degree of deformation are affected by the viscosity of the milling solvent. With the high viscous solvent, the fewest number of collisions, the lowest degree of fracturing, and the lowest degree of deformation are obtained, then, the graphene sheets were obtained with large number of layers whereby the sheets seem to be clear with less defects. On the other hand, with the low viscous solvent, the high number of collisions, the high degree of fracturing and the high degree of deformation are obtained, then, the graphene sheets were obtained with a fewer number of layers thereby the sheets seem to be turbid with high defects.

Morphological and structural characteristics of graphite powders

Morphological characteristics of graphite powders were investigated via scanning electron microscope (SEM) Fig. 1a, at which SEM image represents the flaky shape of graphite powders used as starting material for milling experiment. This image also reveals that the size of the graphite flakes seems to be less than 20 μm with rough surfaces. X-ray diffraction analysis Fig. 1b, was performed to study the structural characteristics of graphite powders, it represents a distinct peak at position of $2\Theta = 26.5°$, this peak is very sharp and intense to confirm the high crystallinity of graphite powders. Raman spectroscopy Fig. 1c, was performed at which Raman spectrum represents three distinct peaks, D band at 1343 cm^{-1}, G band at 1576.3 cm^{-1} and 2D band at 2708.8 cm^{-1} with relative intensity 13.7, 68,3 and 32,8 respectively. The very low D band indicates that the starting graphite has relatively good graphitic structure.

Structural investigations of graphene sheets

XRD analysis of graphene sheets

Structural analyses of the graphene sheets obtained via wet milling of graphite in 2-ethylhexanol and kerosene were performed using X-ray diffraction analysis. Fig. 2, represents XRD patterns of the prepared samples, the XRD pattern of graphene has a strong peak at $2\Theta = 25–27°$ [28]. The distinct peaks of graphene obtained via wet milling in 2-ethyl-hexanol and kerosene are shown at positions of $2\Theta = 26.62°$ and 26.22° respectively.

In comparison to XRD pattern of bulk graphite; the XRD patterns of graphene sheets represent distinct peaks which seem to be very broad with lower intensity especially for the sample obtained with kerosene. According to the presented XRD patterns, the diffraction peaks recorded with the samples prepared in 2-ethyl-hexanol and kerosene seem to be alike in the broadening and intensity. They are very broad and very low which might be due to high reduction in the crystal size occurred as a result of excessive milling time (60 h) integrated with high energy of milling represented by milling speed (400 rpm) and ball to powder ratio (50) in the presence of milling solvent.

Raman spectroscopy of graphene sheets

Raman spectroscopy is a fast and non-destructive technique for providing a direct insight on the electron–phonon interactions, which implies a high sensitivity to electronic and crystallographic structures [10]. Carbon materials show their fingerprints under Raman spectroscopy typically by D, G, and 2D peaks around 1350 cm^{-1}, 1580 cm^{-1} and 2700 cm^{-1} respectively due to the change in electron bands [8].

The D band is recognized as the disorder, or defect band. The band is extremely weak in graphite and high-quality graphene. D band intensity is directly proportional to the level of defects [29]. Here, Raman spectrum Fig. 3, of graphene sheets prepared using 2-ethylhexanol represents that the D band at position 1345.4 cm^{-1} with intensity = 43.5 to indicate valuable amount of defects occurred as a result of high energy milling. On the other hand, Raman spectrum of graphene sheets prepared using kerosene to represent that the D band at position 1347.8 cm^{-1} with intensity = 65.4 indicating the increasing of defect degree. The lowest degree of defects was established via milling in 2-ethylhexanol due to high viscosity that is about 10.3 centipoise against 1.64 centipoise for kerosene in which the highest degree of viscosity diminishes the destructive exfoliation by soft sliding of graphite layers. On the other hand, the highest degree of defects was performed by milling in kerosene as a result of the low viscosity of kerosene. Consequently, the increasing of destructive exfoliation was found and confirmed by the broadening, low intensity represented in the XRD pattern Fig. 2.

The G band is an in-plane vibrational mode concerning sp^2 hybridized carbon atoms that comprise graphene sheets. Its

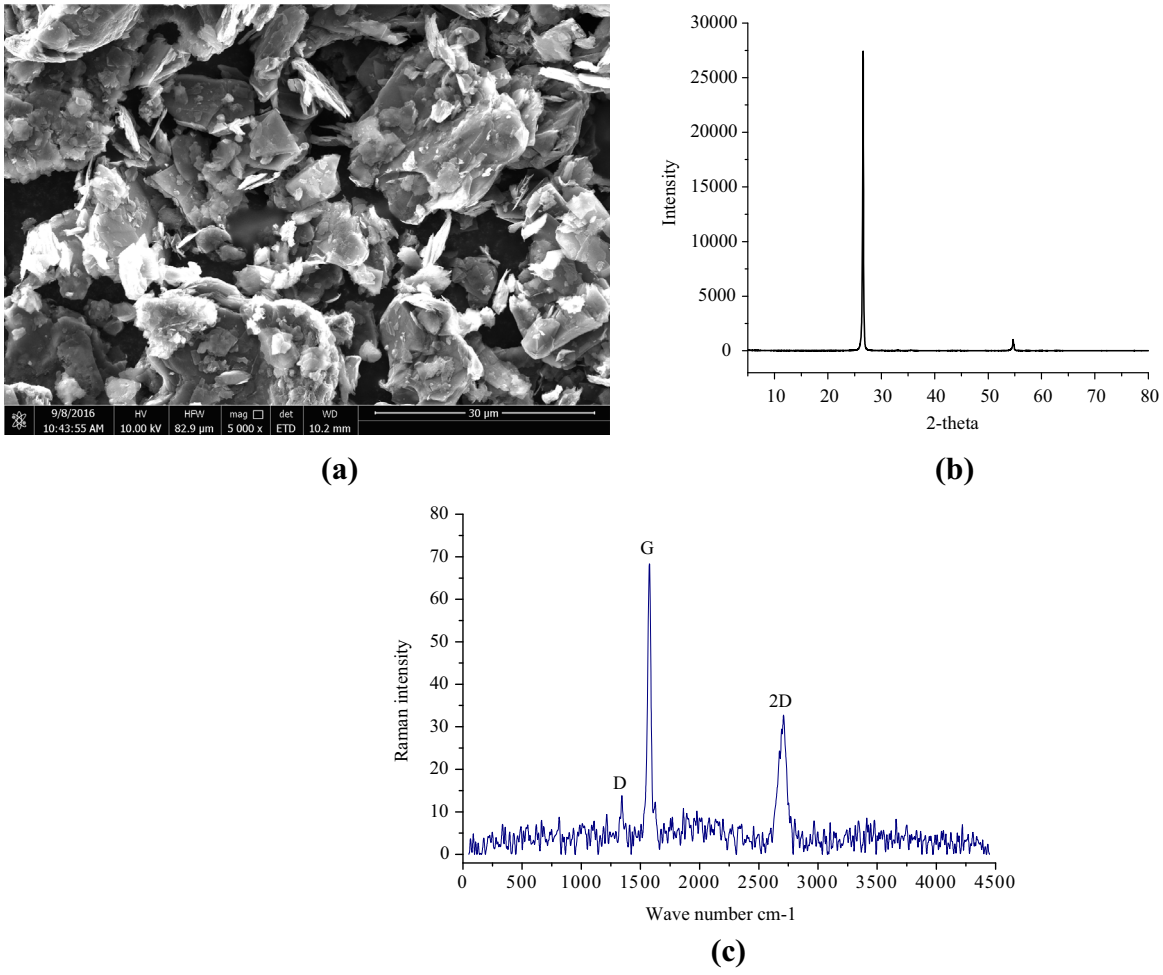

Fig. 1 (a) SEM image, (b) XRD pattern and (c) Raman spectrum of bulk graphite powders.

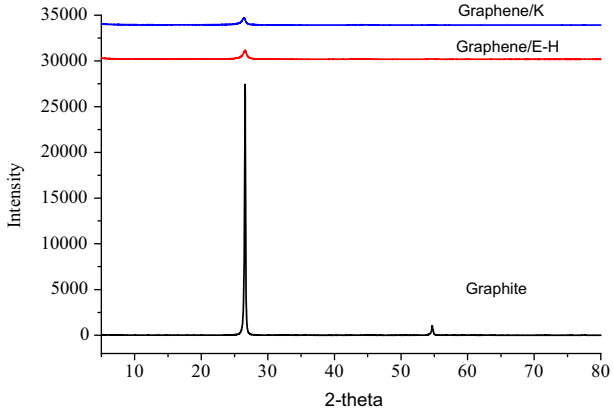

Fig. 2 XRD patterns of graphene sheets versus bulk graphite.

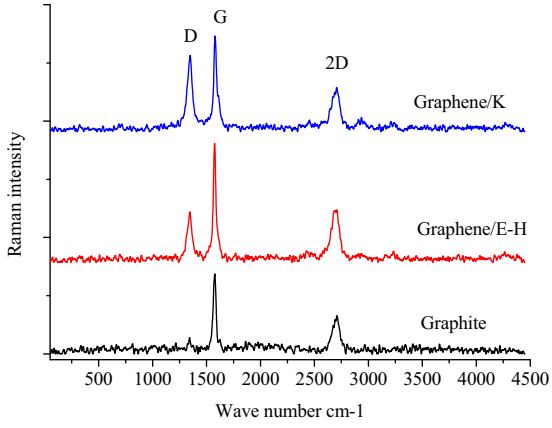

Fig. 3 Raman spectra of bulk graphite versus graphene sheets exfoliated via wet milling in 2-ethylhexanol (E-H) and kerosene (K).

examination allows precise indication of layer thickness. The band position shifts to lesser energy as layer thickness increases, demonstrating a slight softening of bonds [29]. Using the ratio of peak intensities I_D/I_G, one can use Raman spectra to characterize the level of disorder in graphene. As the disorder in graphene increases, I_D/I_G displays 2 different behaviors. There is a regime of "low" defect density where I_D/I_G will increase as a higher defect density creates a more elastic scattering. This occurs up to a regime of "high" defect density, at which point I_D/I_G will begin to decrease as an increasing defect density represents in a more amorphous carbon structure, attenuating all Raman peaks. These two regimes are

referred to as "nanocrystalline carbon" and "mainly sp^2 amorphous carbon" phases, respectively [12]. Then, it is found that, as the structure changes from graphite to nanocrystalline graphite, the ratio between the intensities of D and G lines, $I_{(D)}/I_{(G)}$, rationalize reciprocally with the size of the crystalline grains or inter defect distance. The highest $I_{(D)}/I_{(G)}$ ratio is also evidence for the structure with highest order [16]. Here, Raman spectrum Fig. 3, of graphene sheets prepared using 2-ethylhexanol represents that the G band at position 1574.7 cm^{-1} with intensity = 102 to indicate valuable degree of crystallinity. On the other hand, Raman spectrum of graphene sheets prepared using kerosene represents that the G band at position 1579 cm^{-1} with intensity = 82. Then, by comparing the $I_{(D)}/I_{(G)}$ ratio of the sample milled in 2-ethylhexanol ~0.43 versus $I_{(D)}/I_{(G)}$ ratio of the sample milled in kerosene ~0.80, it was found that the highest order, the lowest crystal size and the fewest number of graphene layers were obtained via wet milling in kerosene. On the other hand, the sample prepared in 2-ethylhexanol represents a shift to the lower position of G peak at 1574.7 cm^{-1} to indicate the increasing of graphene layers which confirmed by the high intensity of G peak at 102. The 2D band is at almost double the frequency of the D band and originates from second order Raman scattering process. This band is used to determine graphene layer thickness. The ratio I_{2D}/I_G for high-quality single-layer graphene is greater than, or equal to 2. This ratio is often used to confirm a defect-free graphene sample [29]. Raman spectrum Fig. 3, of graphene sheets prepared using 2-ethylhexanol represents the 2D band at position 2707.5 cm^{-1} with intensity = 45, and the ratio I_{2D}/I_G = 0.44 while the Raman spectrum of graphene sheets prepared using kerosene represents the 2D band at position 2706.5 cm^{-1} with inten-

Table 1 Positions and relative intensities of D, G, and 2D bands of graphene prepared using wet milling in 2-ethylhexanol against graphene prepared using wet milling in kerosene.

Sample	D band		G band		2D band		I_D/I_G	I_{2D}/I_G
	Position (cm^{-1})	Intensity	Position (cm^{-1})	Intensity	Position (cm^{-1})	Intensity		
GR/E-H	1345.4	43.5	1574.7	102	2707.5	45	0.43	0.44
GR/K	1347.8	65.4	1579	82	2706.5	38	0.80	0.46

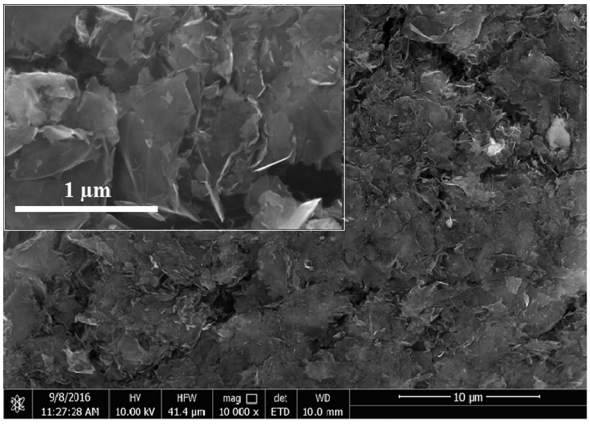

(a)

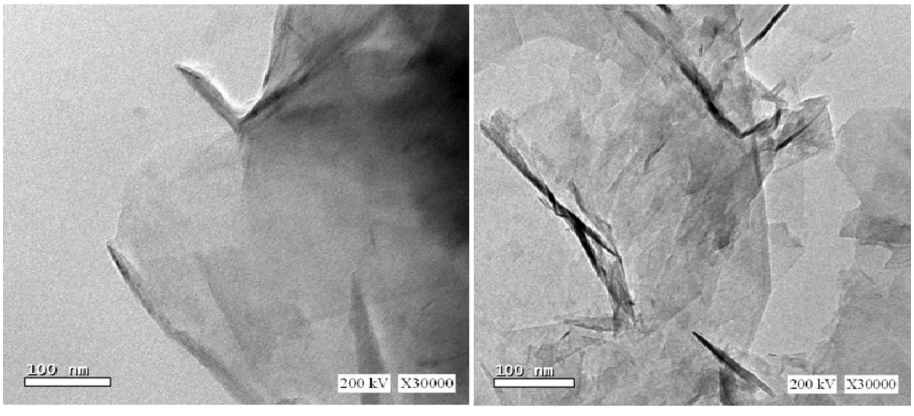

(b)

Fig. 4 (a) SEM and (b) TEM images of graphene sheets prepared via wet milling in 2-ethyl-hexanol.

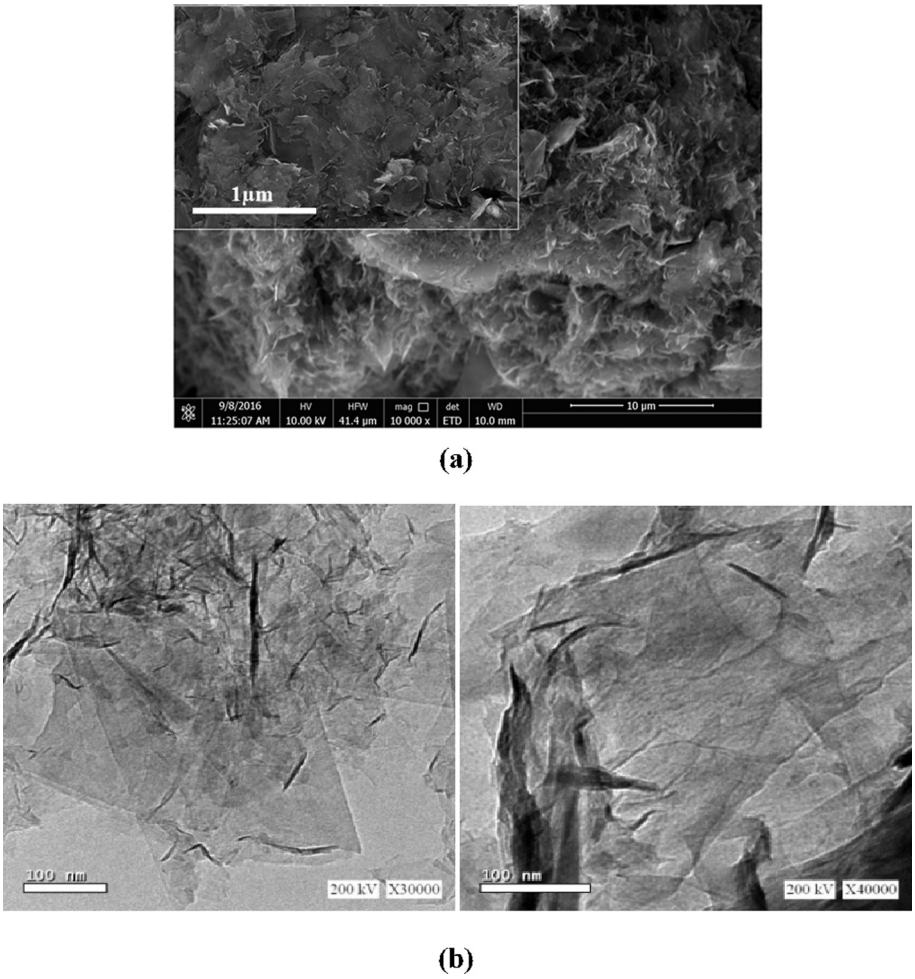

Fig. 5 (a) SEM and (b) TEM images of graphene sheets prepared via wet milling in kerosene.

sity = 35, and the ratio I_{2D}/I_G = 0.46. Consequently, this ratio confirms the highest amount of defects and the largest number of graphene layers. Generally, the presence of all bands with valuable intensities indicates the good graphitic structure of graphene sheets (see Table 1).

Morphological investigations of graphene sheets

Morphological characteristics of the prepared graphene sheets were investigated by scanning electron microscope (SEM) and transmission electron microscope TEM. Figs. 4a, and 5a, represent SEM images of graphene sheets obtained using wet milling in 2-ethylhexanol and kerosene respectively. It can be seen from the images in the frame of these figures that the top-view SEM images reveal that graphene sheets have a lamellar structure with a lateral size smaller than 1 µm, in which the graphene sheets seem to be aggregated layers in a cluster form which might be due to heat treatment at 600 °C.

On the other hand, Figs. 4b, and 5b, represent TEM images of graphene sheets obtained via wet milling in 2-ethylhexanol and kerosene respectively. The sample obtained using wet milling in 2-ethylhexanol represents a good appearance of graphene sheets that are transparent and closed to each other to form many layers representing some folding. On the other hand, TEM images of the sample obtained via wet milling in kerosene, reveal the high deformation of graphene sheets due to milling process in kerosene and represents the small size of the prepared sheets. That high deformation was already confirmed by Raman spectroscopy results.

Conclusions

High energy wet milling was successfully employed to exfoliate graphene sheets from bulk graphite. The exfoliatin process was performed in the presence of two different milling solvents such 2-ethylhexanol and kerosene. The exfoliated grapphene sheets own a good graphitic structure with a large number of graphene layers. The highest level of defects, the fewest number of graphene layers and the smallest crystal size were found in the sample prepared in the presence of kerosene. On the other hand, the lowest level of defects, the largest number of graphene layers, and the largest crystal size were found in the sample prepared using 2-ethylhexanol.

Conflict of Interest

The authors have declared no conflict of interest.

Compliance with Ethics Requirements

This article does not contain any studies with human or animal subjects.

References

[1] Deng J, You Y, Sahajwalla V, Joshi RK. Transforming waste into carbon-based nanomaterials – review. J Carbon 2016;96:105–15.
[2] Terzopoulou Z, Kyzas GZ, Bikiaris DN. Recent advances in nanocomposite materials of graphene derivatives with polysaccharides. Materials 2015;8:652–83.
[3] McAllister MJ, Li J-L, Adamson DH, Schniepp HC, Abdala AA, Liu J, et al. Single sheet functionalized graphene by oxidation and thermal expansion of graphite. Chem Mater 2007;19:4396–404.
[4] Stankovich S, Dikin DA, Piner RD, Kohlhaas KA, Kleinhammes A, Jia Y, et al. Synthesis of graphene-based nanosheets via chemical reduction of exfoliated graphite oxide. Carbon 2007;45:1558–65.
[5] MeiJiao L, Jing L, Xuyu Y, Changan Z, Jia Y, Hao H, et al. Applications of graphene-based materials in environmental protection and detection. Chin Sci Bull 2013;58:2698–710.
[6] Pimenta MA, Dresselhaus G, Dresselhaus MS, Cancado LG, Jorio A, Saito R. Studying disorder in graphite-based systems by Raman spectroscopy. Phys Chem Chem Phys 2007;9:1276–91.
[7] Beams R, Cancado LG, Novotny L. Raman characterization of defects and dopants in graphene. J Phys: Condens Matter 2015;27:083002.
[8] Wahab HS, Ali SH, Abdul-Hussein AM. Synthesis and characterization of graphene by Raman Spectroscopy. J Mater Sci Appl 2015;1(3):130–5.
[9] Ferrari AC. Raman spectroscopy of graphene and graphite: disorder, electron–phonon coupling, doping and nonadiabatic effects. Solid State Commun 2007;143:47–57.
[10] Soldano C, Mahmood A, Dujardin E. Production, properties and potential of graphene.. Carbon 2010;48:2127–50.
[11] Park JS, Reina A, Saito R, Kong J, Dresselhaus G, Dresselhaus MS. G′ band Raman spectra of single double and triple layer graphene. Carbon 2009;47:1303–10.
[12] Xing T, Li LH, Hou L, Hu X, Zhouet S, Peteral R, et al. Disorder in ball-milled graphite revealed by Raman spectroscopy. Carbon 2013;57:515–9.
[13] Singh V, Joung D, Zhai L, Das S, Khondaker SI, Seal S. Graphene based materials: past, present and future. Prog Mater Sci 2011;56:1178–271.
[14] Yang Y, Shi W, Zhang R, Luan C, Zeng Q, Wang C, et al. Electrochemical exfoliation of graphite into nitrogen-doped graphene in glycine solution and its energy storage properties. Electrochim Acta 2016;204:100–7.
[15] Yang Y, Lu F, Zhou Z, Song W, Chen Q, Ji X. Electrochemically cathodic exfoliation of graphene sheets in room temperature ionic iiquids N-butyl, methylpyrrolidinium bis (trifluoromethylsulfonyl) imide and their electrochemical properties. Electrochim Acta 2013;113:9–16.
[16] Sundaram RS. Chemically derived graphene. In: Skakalova V, Kaiser AB, editors. Graphene. Woodhead Publishing; 2014. p. 50–80.
[17] Frank O, Kalbac M. Chemical vapor deposition (CVD) growth of graphene films. In: Skakalova V, Kaiser AB, editors. Graphene. Woodhead Publishing; 2014. p. 27–49.
[18] Liu W, Li H, Xu Ch, Khatami Y, Banerjee K. Synthesis of high-quality monolayer and bilayer graphene on copper using chemical vapor deposition. Carbon 2011;49:4122–30.
[19] First PN, De Heer WA, Seyller T, Berger C. Epitaxial graphenes on silicon carbide. MRS Bull 2010;35(04):296–305.
[20] Subrahmanyam K, Panchakarla LS, Govindaraj A, Rao CNR. Simple method of preparing graphene flakes by an arc-discharge method. J Phys Chem C 2009;113(11):4257–9.
[21] Edwards RS, Coleman KS. Graphene synthesis: relationship to applications. Nanoscale 2013;5(1):38–51.
[22] Zhou M, Tian T, Li X, Sun X, Zhang J, Cui P, et al. Production of graphene by liquid-phase exfoliation of intercalated graphite. Int J Electrochem Sci 2014;9:810–20.
[23] Zhao W, Wu F, Wu H, Chen G. Preparation of colloidal dispersions of graphene sheets in organic solvents by using ball milling. J Nanomater 2010;155:1–5.
[24] Fan X, Chang DW, Chen X, Baek J, Dai L. Functionalized graphene nanoplatelets from ball milling for energy applications. Curr Opin Chem Eng 2016;11:52–8.
[25] Kumar GR, Jayasankar K, Das SK, Dash T, Dash A, Jena BK, et al. Shear-force-dominated dual-drive planetary ball milling for the scalable production of graphene and its electrocatalytic application with Pd nanostructures. RSC Adv 2016;6:20067–73.
[26] Jeon I-Y, Shin YR, Sohn G-J, Choi H-J, Bae S-Y, Mahmood J, et al. Edge-carboxylated graphene nanosheets via ball milling. PNAS 2012;109(15):5588–93.
[27] Liu L, Xiong Z, Hu D, Wu G, Chen P. Production of high quality single- or few-layered graphene by solid exfoliation of graphite in the presence of ammonia borane. Chem Commun 2013;49:7890–2.
[28] Seresht RJ, Jahanshahi M, Rashidi AM, Ghoreyshi AA. Synthesis and characterization of thermally-reduced graphene. Iranica J Energy Environ 2013;4(1):53–9.
[29] Wall M. Raman Spectroscopy optimizes graphene characterization: Raman spectroscopy is an indispensable tool. Adv Mater Process; April 2012 Issue.